GaAs HOMOJUNCTION SOLAR CELL DEVELOPMENT

Dennis J. Flood, Clifford K. Swartz,
and Russell E. Hart, Jr.
NASA Lewis Research Center
Cleveland, Ohio

SUMMARY

The Lincoln Laboratory $n^+/p/p^+$ GaAs shallow homojunction cell structure (ref. 1) has been successfully demonstrated on 2- by 2-cm GaAs substrates (ref. 2). Air mass zero efficiencies of the seven cells produced to date have ranged from 13.6 to 15.6 percent. Current-voltage (I-V) characteristics, spectral response, and I_{sc}-V_{oc} measurements have been made on all seven cells. Preliminary analysis of 1-MeV electron radiation damage data indicate excellent radiation resistance for these cells.

INTRODUCTION

The compound semiconductor GaAs has several physical properties that make it a potentially useful material for space solar-cell applications. Because GaAs has a direct band gap, the absorption length for near band gap sunlight in a single-crystal of the material is only about 2 μm (ref. 3), or approximately a factor of 100 shorter than that in silicon. As a result, the solar-cell active layer thickness can be reduced to a few micrometers. In addition, GaAs solar cells should exhibit excellent radiation resistance in space since, in principle, it is possible to have minority carrier diffusion lengths that are several times greater than the absorption length. As a result, photocurrent collection should not be significantly affected until relatively large space radiation fluences have been accumulated. Radiation damage data for GaAs solar cells in general are sparse, although results for the LPE (liquid-phase epitaxy) -grown p/n heteroface cell are becoming more available (e.g., refs. 4 to 8). By comparison, data on the VPE (vapor-phase epitaxy) -grown $n^+/p/p^+$ shallow homojunction cells exist only for relatively small area (0.5 cm^2) cells (ref. 9). In the present work six 2- by 2-cm cells, fabricated at the Lincoln Laboratory under NASA Lewis Contract C-30969-D, have been irradiated with 1-MeV electrons at five fluences from 10^{13} to 10^{15} e^-/cm^2. Current-voltage, spectral response, and I_{sc}-V_{oc} measurements were made on each cell after each irradiation. The irradiations were performed using the Lewis Research Center's Dynamitron Accelerator.

RESULTS AND DISCUSSION

Table I contains the pre-irradiation values of short-circuit current I_{SC}, open-circuit voltage V_{OC}, maximum power P_m, fill factor FF, and AMO efficiency η of each of the cells used in this study. All cells have 0.05-μm-thick n^+ layers doped with sulfur to ~5×10^{18} cm^{-3}, 0.085-μm-thick anodic oxide antireflection (AR) coatings, electroplated tin contacts on the front surface, and an electroplated gold contact on the back surface. Thicknesses of the p and p^+ regions varied from cell to cell, as did the zinc concentration in the p region. The p^+ region, also zinc doped, is approximately the same for all cells at 5×10^{18} cm^{-3}. Figure 1 shows the basic cell structure without AR coating and contacts.

Figure 2 is a plot of normalized short-circuit current as a function of fluence for the best and worst cases among the six cells. Degradation after 10^{15} e^-/cm^2 1-MeV electrons ranged from 10 to 20 percent of beginning-of-life (BOL) currents. Spectral response measurements show clearly that, as expected, degradation occurs only at the longer wavelengths (see fig. 3). Figure 4 is a plot of normalized open-circuit voltage as a function of fluence again for the same two cells of figure 1. As shown, the cell with the least current degradation exhibits the greatest voltage degradation, a result not yet fully understood. Relative degradation after $\phi = 10^{15}$ ranged from 9 to 16 percent for the six cells. The degradation of normalized maximum power is shown in figure 5. Relative degradation ranged from 24 percent in the best case to 30 percent in the worst case at the maximum fluence. Figure 6(a) contains the I-V characteristics at $\phi = 0$ and $\phi = 10^{15}$ e^-/cm^2 for the cell with the greatest degradation in I_{SC}. As shown in the figure, there was a slight decrease in fill factor at the highest fluence. Figure 6(b) contains the I-V characteristics for the cell with the least degradation in I_{SC} (and P_m) for comparison. Figure 7 is a typical plot of I_{SC} versus V_{OC} for the cells used in this study at $\phi = 0$ and 10^{15} e^-/cm^2. Shunt resistances were typically on the order of 10^6 ohms for these cells. Figure 8 is a plot of I_{SC}-V_{OC} for cell 5426. The I_{SC}-V_{OC} data are obtained by varying the intensity of the light source to obtain a range of short-circuit currents comparable to dark forward bias currents. The data are thus automatically corrected for the series resistance of the cell. The data of figure 8 indicate a large current in the generation-recombination regime of the I_{SC}-V_{OC} characteristic. The shunt resistance of this cell was estimated to be on the order of 500 ohms.

Figure 9 is a plot of the electron damage coefficient for p-type GaAs as a function of p-layer doping density, calculated from electron radiation damage data to small-area, shallow-homojunction cells (ref. 2). Similar calculations are in progress with data obtained from the 2- by 2-cm cells of this work, and indicate agreement with the data of figure 9.

CONCLUSION

The shallow homojunction $n^+/p/p^+$ GaAs solar cells tested in this study show good resistance to 1-MeV electron irradiation. Although the $n^+/p/p^+$ structure has not yet been optimized for maximum BOL performance and maximum radiation resistance, cells produced to date are comparable to the best GaAs p/n cells of similar BOL efficiencies. Careful attention to optimization of the cell structure should yield cells with improved radiation resistance over the cells reported here.

REFERENCES

1. Bozler, C. O.; and Fan, J. C. C.: High Efficiency GaAs Shallow-Homojunction Solar Cells. Appl. Phys. Lett., vol. 31, Nov. 1, 1977, pp. 629-631.

2. Fan, J. C. C.: GaAs Shallow Homojunction Solar Cells. NASA CR-165167, October 1980.

3. Kamath, S.; and Wolff, G.: High Efficiency GaAs Solar Cell Development. AFAPL-TR-78-96, Hughes Aircraft, 1979. (Available from NTIS as AD-A066616.)

4. Loo, R.; Kamath, G. S.; and Knechtli, R.: Electron Radiation Damage of (AlGa)As-GaAs Solar Cells. NASA CR-162425, 1979.

5. Conway, E. J.; and Walker, G. H.: Radiation Damage in GaAs Solar Cells. Solar Cell High Efficiency and Radiation Damage - 1979. NASA CP-2097, 1979, pp. 201-207.

6. Moon, R. L.; et al.: Performance of AlGaAs/GaAs Solar Cells in the Space Environment. 12th Photovoltaic Specialists Conference Record. IEEE, 1976, pp. 255-261.

7. Pearce, L. S.; et al.: Proton and Electron Irradiation of Liquid Phase Epitaxial GaAlAs Solar Cells. Photovoltaic Specialists Conference, 13th, Washington, D.C., June 1978, Conference Record. IEEE, 1978, pp. 557-561.

8. Li, Sheng S.; et al.: Effects of Thermal Annealing on the Deep-Level Defects and I-V Characteristics of 200 KeV Proton Irradiated AlGaAs-GaAs Solar Cells. Energy to the 21st. Century; Proceedings of the Fifteenth Intersociety Energy Conversion Engineering Conference. Vol. I. AIAA, 1980, pp. 354-357.

9. Fan, J. C. C.; Chapman, R. L.; and Bozler, C. O.: Shallow-Homojunction GaAs Cells with High Resistance to 1-MeV Electron Radiation. Appl. Phys. Lett., vol. 36, Jan. 1, 1980, pp. 53-56.

TABLE I. - CELL PARAMETERS

Cell	Short-circuit current, I_{sc}, A	Open-circuit voltage, V_{oc}	Maximum power, P_m, mW	Fill factor, FF	Air mass zero efficiency, η, percent
5239	0.1088	0.961	81.82	78.2	14.9
5245	.1034	.983	82.56	81.2	15.1
5340	.0976	.970	73.56	77.7	13.4
5344	.1074	.984	85.46	80.8	15.6
5348	.1020	.992	82.40	81.4	15.0
5426	.1045	.987	80.90	78.4	14.8

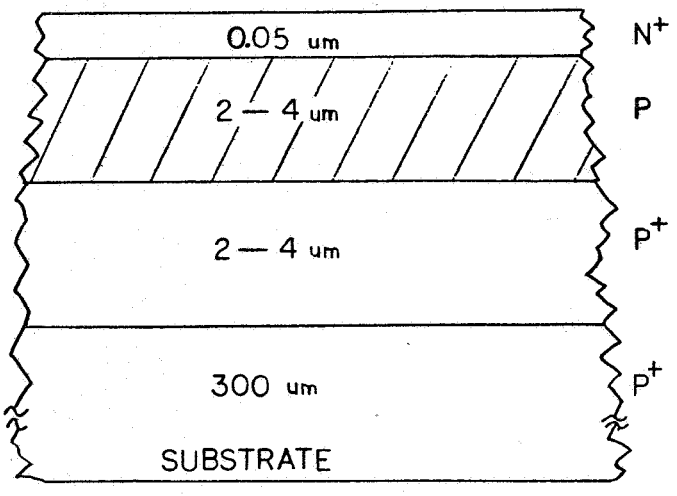

FIGURE I. SHALLOW HOMOJUNCTION CELL STRUCTURE.

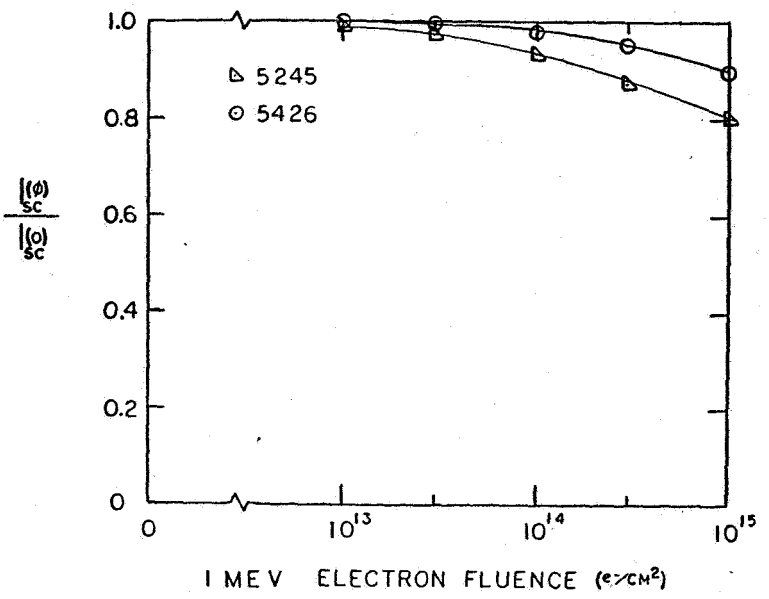

FIGURE 2. SHORT-CIRCUIT CURRENT DEGRADATION (NORMALIZED).

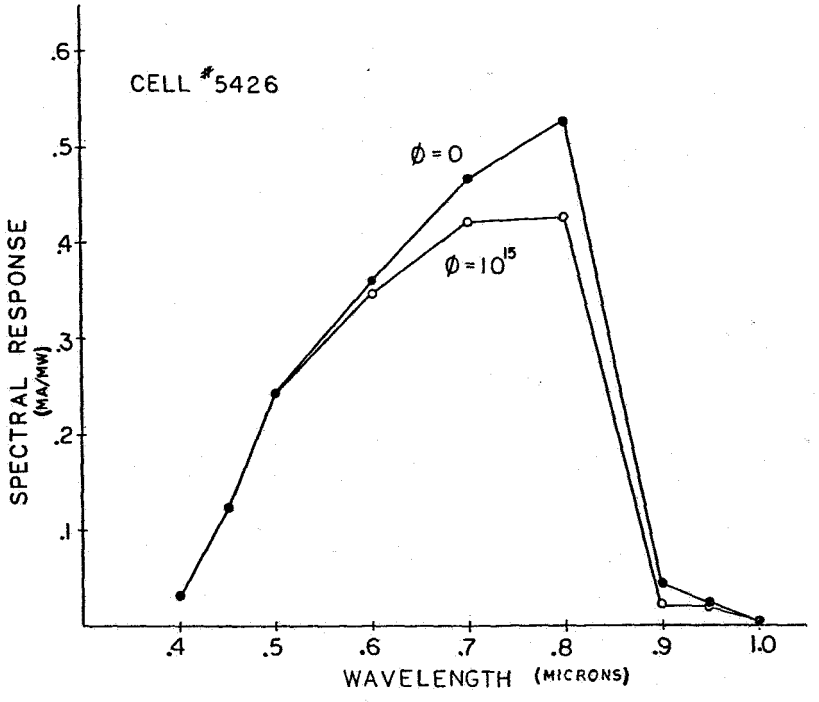

FIGURE 3. SPECTRAL RESPONSE, $N^+/P/P^+$ GAAS CELL.

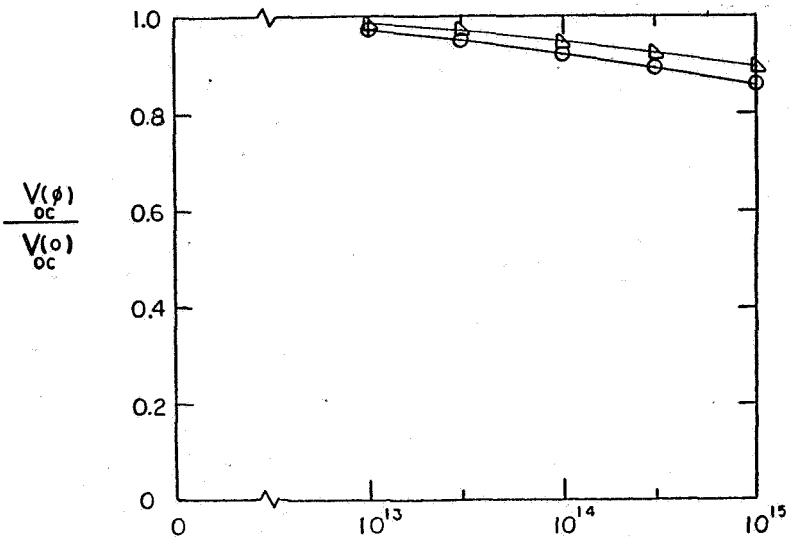

FIGURE 4. OPEN CIRCUIT VOLTAGE DEGRADATION (NORMALIZED).

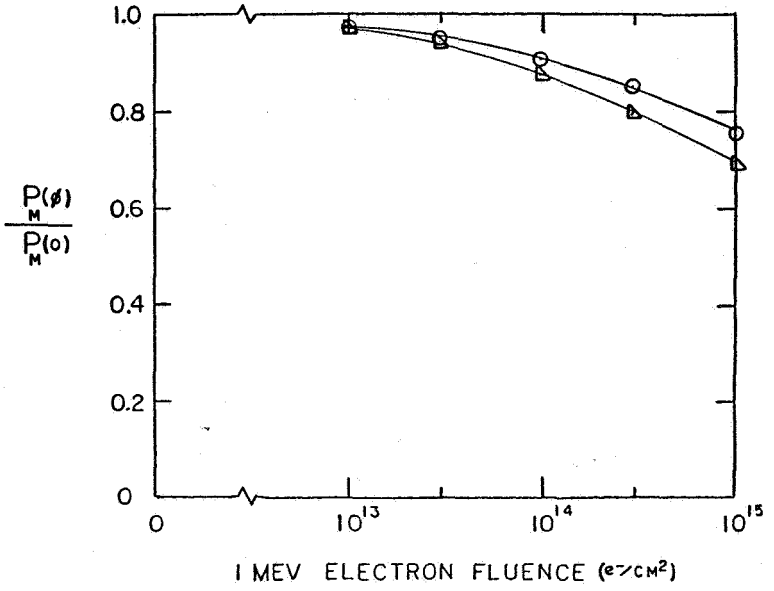

FIGURE 5. MAXIMUM POWER DEGRADATION (NORMALIZED).

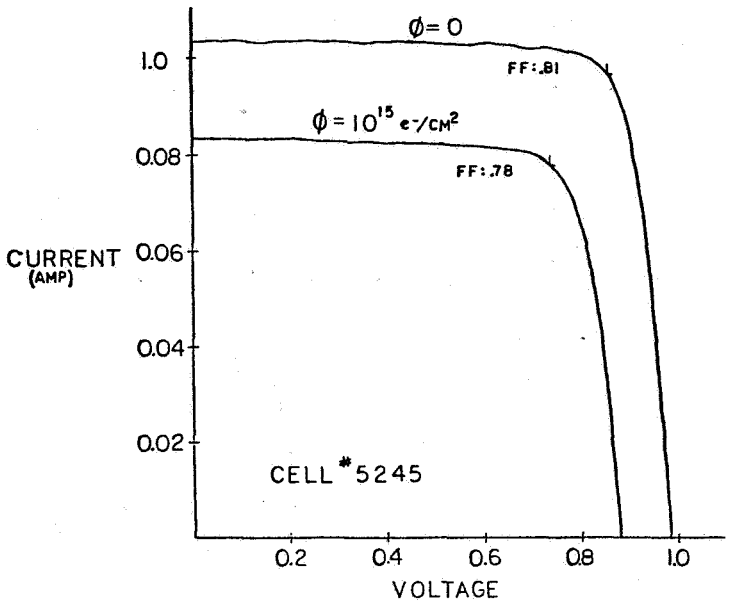

FIGURE 6a. CURRENT-VOLTAGE CHACTERISTICS, "WORST CELL".

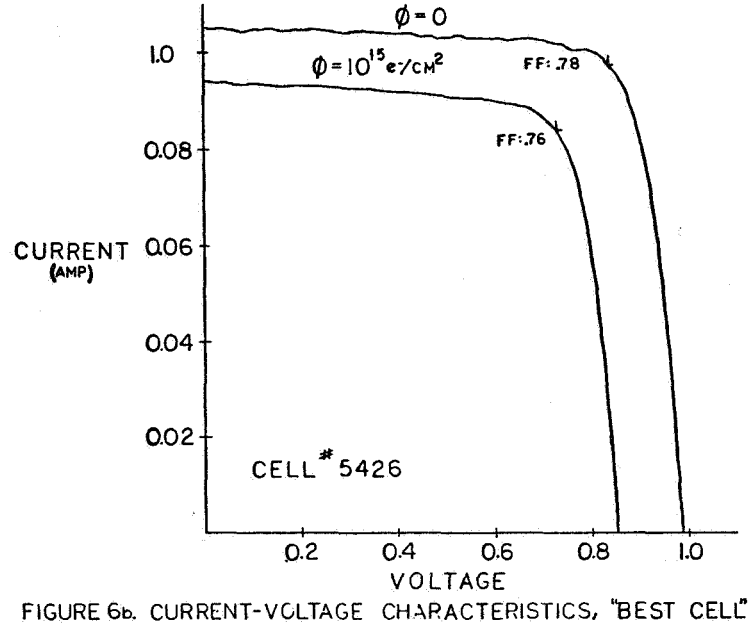

FIGURE 6b. CURRENT-VOLTAGE CHARACTERISTICS, "BEST CELL"

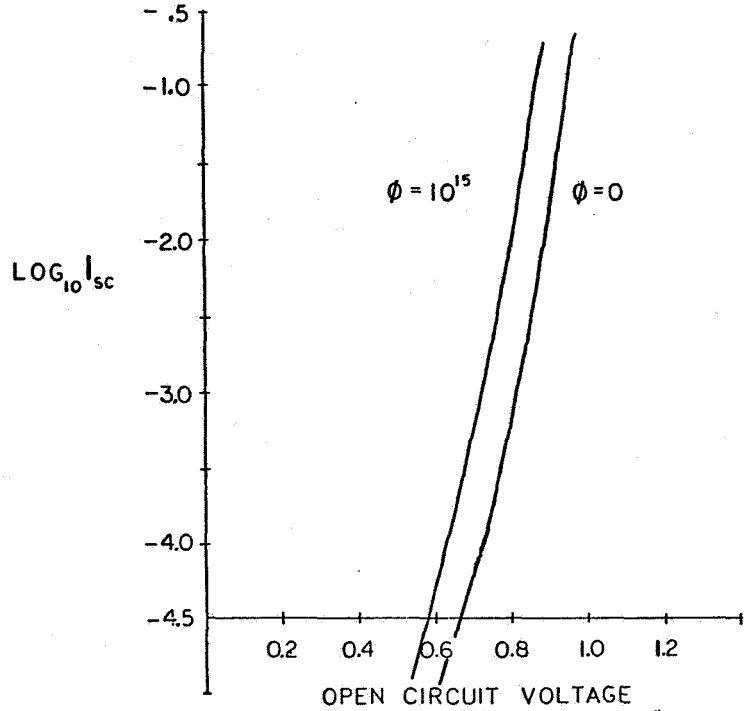

FIGURE 7. I_{sc}-V_{oc} CHARACTERISTICS, "TYPICAL CELL".

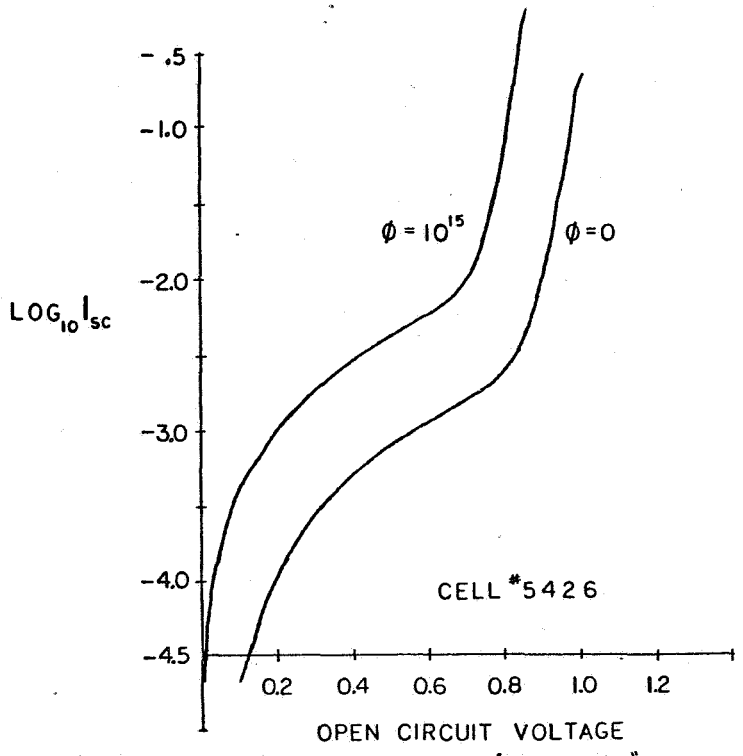

FIGURE 8. I_{sc}-V_{oc} CHARACTERISTICS, "BEST CELL".

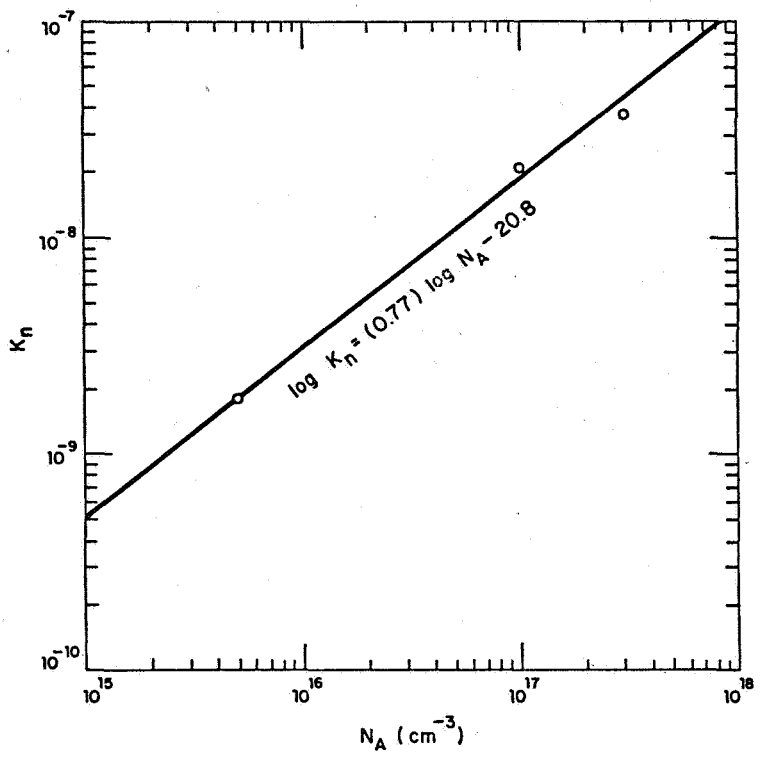

Figure 9. A plot of damage coefficient $K_n\phi$ as a function of doping levels in p-type GaAs.